Slow dynamics and aging in a constrained diffusion model

Federico Corberi,[1] Mario Nicodemi,[2,3] Marina Piccioni,[3] and Antonio Coniglio[3]
[1]*Dipartimento di Fisica, Universitá di Salerno, and Istituto Nazionale per la Fisica della Materia, Unitá di Salerno, 84081 Baronissi (Salerno), Italy*
[2]*Department of Mathematics, Imperial College, Huxley Building, 180 Queen's Gate, London, SW7 2BZ, United Kingdom*
[3]*Dipartimento di Scienze Fisiche, Universitàà di Napoli and Istituto Nazionale di Fisica della Materia, Unitàà di Napoli, Mostra d'Oltremare, Pad. 19, 80125 Napoli, Italy*
(Received 20 July 2000; published 23 February 2001)

We carry out a complete analysis of the schematic diffusive model recently introduced for the description of supercooled liquids and glassy systems above the glass temperature. The model is described by a trivial equilibrium measure and the presence of kinetics constraints is mimicked through a rapidly decreasing mobility at high particle density. The governing equation describing a sudden quench process is investigated analytically in a mean field approach and by means of numerical simulations. For deep quenches a long lasting off-equilibrium dynamics is observed in dense systems before equilibration is achieved, where time translational invariance lacks and the system ages. The kinetics is slow in this time domain since the average particle diffusivity D decreases in time, as opposed to the standard diffusion case of a constant D, that is recovered only in equilibrium. The autocorrelation function decays slower than an exponential, falling in mean field as an enhanced power law. The linear response function is computed and the modalities of the break-down of the fluctuation dissipation theorem are analytically investigated, showing that an *effective* temperature can be defined which slowly approaches the bath temperature from above.

DOI: 10.1103/PhysRevE.63.031106 PACS number(s): 05.40.−a, 05.70.Ln, 75.40.Gb

I. INTRODUCTION

When glass-forming liquids are supercooled below the melting temperature their dynamical properties undergo dramatic changes and, in particular, the equilibrium relaxation time τ_0 increases of several orders of magnitude. The schematic scenario about the microscopic origin of this slowing down is generally believed to be the following: a particle does not perform a Brownian motion in the fluid but rattles many times inside *cages* formed by the surrounding molecules. The motion of a particle over distances larger than the typical cage size is severely suppressed when the density is high because configurational restrictions require a cooperative rearrangement of many particles and a *complex* slow dynamics is originated. Hard spheres are known [2] to reproduce these features and can be considered, therefore, as a simple paradigm: kinetic constraints are themselves responsible for dynamical features, the equilibrium measure being, in this case, trivial. Thermodynamic observables are, in general, rather regular along the glass transformation of many systems. When the characteristic duration τ_0 of this cooperative process exceeds the observation time the glass appears out of equilibrium. Structural rearrangements in this case become slower and slower as time goes on and the system ages. Time translational invariance (TTI) is lost and the response to an external perturbation depends on the *age* of the system, that is the time elapsed since its preparation. The fluctuation-dissipation theorem (FDT) is thus violated.

In the main approach to glassy kinetics, the mode coupling theory [3], the dynamical equations are solved by resumming a nontrivial set of diagrams and a glass transition appears as a purely dynamical effect. This theory predicts an equilibration time τ_0 which diverges as a power law at the dynamical transition. Today it is well established [2] that the quoted theory applies in a region located well before the ideal glass point, where τ_0 is found experimentally to diverge according to the Vogel-Fulcher law [2]

$$\tau_0 \sim \exp[v(\rho_c - \overline{\rho})^{-1}], \tag{1}$$

where $\overline{\rho}$ and ρ_c are the average particle density, and the critical density, respectively. Therefore we do not have information from the theoretical point of view on the dynamical behavior close to the glassy transition where standard theories do not apply. However, since glassy features are mainly of a kinetic nature, it is important to establish how them depend on the details of the dynamics.

In a recent paper [1], a simple diffusive model has been introduced to describe the slow relaxation process in supercooled fluids near the dynamical transition and related glassy systems. The model aims to describe the main features of the out-of-equilibrium dynamics above the temperature of structural arrest. It is schematic in spirit and, in order to be generic, leaves aside as much system specific details as possible. The basic assumption is that a good deal of the complex behavior observed in glassy systems can be encoded into a conventional diffusion equation by means of a suitably chosen particle mobility M. Since particle motion in real systems is severely suppressed in high density regions, due to kinetic constraints, the mobility is assumed to be a decreasing function of the density that vanishes as an arrest density ρ_c is approached. These being the only ingredients, the model appears to be in the spirit of the Kob and Andersen model [4], although the present approach is in the continuum. M is chosen phenomenologically in order to reproduce the relaxation time (1) observed in this region. The same form of M, however, has been obtained by several authors in apparently heterogeneous contexts such as car park-

ing problems [5] or free volume theories of the glass transition [6] (a sketch of this approach is given in Appendix B). The advantage of the present model is in its generality and simplicity, which allows one to compute the behavior of different observables by numerical simulations or analytically in a mean field approximation.

In this paper a quench process is considered: a system in equilibrium at a very high temperature is suddenly brought to a very low temperature. Our main result is the observation of a long lasting preasymptotic aging dynamics, before the equilibrium state is entered. In this preasymptotic time domain the system evolves out of an initially pinned state, which is due to the cage effect, by means of a slow dynamics characterized by a progressive decrease of the particle mobility. This glassy behavior is due to the existence of many time scales because dense regions are almost frozen and evolve slowly whereas less dense regions proceed quickly towards local equilibration. In this regime the autocorrelation function decays slower than exponentially, falling as an enhanced power law in mean field. Both TTI and the FDT are violated, the system being far from equilibrium. In mean field the modalities of the FDT break down can be analytically considered and an *effective* temperature of the system can be introduced which slowly approaches the bath temperature from above.

The plan of the paper is as follows. In Sec. II the model kinetic equation is introduced. In Sec. III the dynamical process is specified by introducing the quench parameters. In Sec. IV the main observables are defined. Section V is devoted to the formulation of the mean field approximation. Section VI presents the analytical solution of the mean field equations. In Sec. VII the breakdown of the FDT is considered in mean field. In Sec. VIII the results of the numerical simulation of the full model are presented. We draw our conclusions in Sec. IX.

II. KINETIC EQUATION

We consider an assembly of particles in a d-dimensional space. This system is described in terms of a coarse-grained variable $\rho(\vec{r})$ representing the average particle density inside a box of typical size a centered at $\vec{r}$. Since the overall number of particles is conserved during the evolution, the dynamics is properly described by a continuity equation

$$\frac{\partial \rho(\vec{r},t)}{\partial t} = -\nabla \cdot \vec{J}\{\rho\} + \eta(\vec{r},t), \tag{2}$$

where the Langevin stochastic term $\eta(\vec{r},t)$, that will be specified below [Eqs. (6)], takes into account the temperature fluctuations. From the chemical potential $\mu\{\rho\}$

$$\mu\{\rho\} = \frac{\partial F\{\rho\}}{\partial \rho}, \tag{3}$$

where $F\{\rho\}$ is the free energy density of the considered system, the current $\vec{J}\{\rho\}$ is obtained [7] as

$$\vec{J}\{\rho\} = -M\{\rho\}\nabla \mu\{\rho\}, \tag{4}$$

where $M\{\rho\}$ is a mobility (we assume that M does not depend explicitly on space, due to homogeneity and isotropy, nor on time because of TTI) that will be discussed below. With Eqs. (2),(4) we arrive at the following diffusion equation for the coarse-grained variable $\rho(\vec{r},t)$:

$$\frac{\partial \rho(\vec{r},t)}{\partial t} = \nabla\left[M\{\rho\}\nabla \frac{\delta F\{\rho\}}{\delta \rho}\right] + \eta(\vec{r},t). \tag{5}$$

According to the fluctuation-dissipation theorem, the expectation values of the noise field $\eta(\vec{r},t)$ are given by

$$\langle \eta(\vec{r},t)\rangle = 0,$$

$$\langle \eta(\vec{r},t)\,\eta(\vec{r}',t')\rangle = -2T\nabla\{M\{\rho\}\nabla[\,\delta(\vec{r}-\vec{r}')\,\delta(t-t')\,]\}, \tag{6}$$

where $\langle \cdots \rangle$ indicates ensemble averages and temperature is measured in units of the Boltzmann constant k_B. Equation (5) is fully specified by assigning the form of $M\{\rho\}$ and of $F\{\rho\}$. With Eq. (5) it will be shown that, for low temperatures, the characteristic relaxation time in the equilibrium state behaves as $M^{-1}(\overline{\rho})$. Then, in order to reproduce the observed behavior (1) of the relaxation time, we consider a phenomenological density-dependent local mobility

$$M(\rho) = \begin{cases} e^{v[\rho(\vec{r},t)-1]^{-1}} & \text{for } \rho \leqslant 1, \\ 0 \quad \text{for } \rho > 1, \end{cases} \tag{7}$$

where ρ_c has been rescaled to unity, for simplicity. A similar form has also been derived in different approximations by several authors [5,6,8]. A sketch of its derivation in the spirit of free volume theories is reported in Appendix B. Regarding the free energy, given that the essence of the glassy behavior is expected to be encoded into the form (7) of the mobility, we consider the simple form appropriate for a gas-lattice model of noninteracting particles

$$\frac{F\{\rho\}}{T} = \int d\vec{r}\{\rho(\vec{r})\ln \rho(\vec{r}) + [1-\rho(\vec{r})]\ln[1-\rho(\vec{r})]\} \tag{8}$$

whose derivation is recalled in Appendix A.

III. QUENCH PROCESSES

Throughout this paper we will concentrate on the dynamics of the model following an instantaneous temperature quench at time $t=0$ from an initial equilibrium state at the temperature T_i to a final lower temperature T. It must be observed that the equilibrium state of the model is completely disordered, for every value of the temperature, since particles are not interacting. However, although the initial and final states are trivial, the dynamical pattern that connects them will be shown to be highly nontrivial.

Cooling experiments on glass-former liquids are always performed with a finite cooling rate r; in this case one usually observes [2] that a large r brings a supercooled liquid out of equilibrium before (at higher temperatures) than for smaller cooling rates. In the present approach it is possible to

take into account the effect of a finite r by introducing a time dependent temperature T in Eqs. (6); this, however, increases the difficulty of the analytic approach that will be discussed in Sec. V. Therefore in the present paper we will only consider the case of an instantaneous quench, living the analysis of a continuous quenching to a forthcoming article. Moreover, it is reasonable to consider a series of instantaneous shallow quenches (i.e., with a small value of $\Delta T = T_i - T$) as a paradigm of a continuous quench with a small cooling rate, whereas a deep quench (with ΔT large) can be regarded as an extrapolation of a case with large r. From the analysis of the dynamical properties of the model that will be made in the following sections, in fact, it will be clear that a markedly out-off-equilibrium behavior is observed in the case of a deep quench, whereas the evolution is always nearby equilibrium for sufficiently shallow quenches.

IV. OBSERVABLES

In this section we introduce the most important observables for the description of the dynamics of Eq. (5), that will be explicitly computed in a mean field approximation in Sec. VI and numerically in Sec. VIII. The main quantity for the study of the time decay of fluctuations is the correlator $C(\vec{k},t_w,t)$, namely the Fourier transform of the real space two-time density-density correlation function. $C(\vec{k},t_w,t)$ is defined by

$$C(\vec{k},t_w,t)=\langle \rho(\vec{k},t_w)\rho(-\vec{k},t)\rangle, \tag{9}$$

where $\rho(\vec{k},t)$ is the Fourier transform of the density field $\rho(\vec{r},t)$. The normalized correlator $\tilde{C}(\vec{k},t_w,t)$, defined by

$$\tilde{C}(\vec{k},t_w,t)=\frac{C(\vec{k},t_w,t)}{C(\vec{k},t_w,t_w)} \tag{10}$$

will be also considered and the (on site) autocorrelation

$$A(t_w,t)=\langle \rho(\vec{r},t_w)\rho(\vec{r},t)\rangle=\int_{|\vec{k}|<\Lambda}\frac{d^dk}{(2\pi)^d}\,\tilde{C}(\vec{k},t_w,t), \tag{11}$$

where Λ is a phenomenological ultraviolet momentum cutoff of order a^{-1}. These quantities are usually studied in numerical simulations and real experiments. The spatial distribution of the density field $\rho(\vec{r},t)$ can be studied through the equal time correlator, the so-called structure factor $C(\vec{k},t,t)$. The existence of inhomogeneities can also be monitored by computing the average squared amount of density fluctuations

$$S^2(t)=\langle[\rho(x,t)-\overline{\rho}]^2\rangle \tag{12}$$

which can be obtained from the knowledge of the structure factor as

$$S^2(t)=(2\pi)^{-d}\int_{|k|<\Lambda}C(\vec{k},t,t)d\vec{k}. \tag{13}$$

Experiments [9] as well as numerical simulations [10] are very often concerned with the behavior of quantities related to the microscopic motions of particles. In the present contest we consider the average diffusivity

$$D(t)=\langle M\{\rho\}\rangle \tag{14}$$

which does not depend on the position, due to space homogeneity. Actually, $D(t)dt$ is the mean distance traveled by a particle in an elementary time step dt so that the quantity $R^2(t)$, defined by

$$R^2(t)=\int_0^t D(t')dt' \tag{15}$$

represents its mean square displacement since the quench time, the motion being diffusive.

V. A MEAN FIELD APPROACH

Equation (5) cannot be solved analytically because of the nonlinearities involved in both $M(\rho)$ and $F\{\rho\}$. In order to make some analytical progress we resort to some approximations that will be shown to provide a description in substantial agreement with the outcomes of the direct numerical integration of Eq. (5) discussed in Sec. VIII.

We introduce a *mean field* approximation on the mobility term by replacing $M(\rho)$ with the effective diffusivity $D(\rho)$ defined in Eq. (14). Equation (5) then becomes

$$\frac{\partial\rho(\vec{r},t)}{\partial t}=D(t)\nabla^2\frac{\partial F\{\rho\}}{\partial\rho}+\eta'(\vec{r},t), \tag{16}$$

where the noise term is a Gaussian random field with expectations

$$\langle\eta'(\vec{r},t)\rangle=0,$$

$$\langle\eta'(\vec{r},t)\,\eta'(\vec{r}',t')\rangle=-2TD(t)\nabla^2[\delta(\vec{r}-\vec{r}')\,\delta(t-t')]. \tag{17}$$

Furthermore, we consider an harmonic approximation for the free energy (8). Expanding the logarithm to lowest order around the average density $\overline{\rho}$ one has

$$F\{\rho\}\simeq\frac{1}{2\overline{\rho}(1-\overline{\rho})}(\rho-\overline{\rho})^2, \tag{18}$$

where constant and linear terms have been discarded since they do not contribute to Eq. (16). Substituting Eq. (18) into Eq. (16) we arrive at

$$\frac{\partial\rho(\vec{r},\tilde{t})}{\partial\tilde{t}}=D(\tilde{t})\nabla^2\rho(\vec{r},\tilde{t})+\tilde{\eta}(\vec{r},\tilde{t}), \tag{19}$$

where a rescaled time $\tilde{t}$ has been introduced

$$\tilde{t}=\frac{1}{\overline{\rho}(1-\overline{\rho})}t \tag{20}$$

and $\tilde{\eta}(\vec{r},t)$ obeys Eqs. (17) with, instead of T, a rescaled temperature $\tilde{T}$ defined by

$$\tilde{T}=\overline{\rho}(1-\overline{\rho})T. \tag{21}$$

In the following we will always drop the tilde from both the rescaled time $\tilde{t}$ and temperature $\tilde{T}$ since this is unambiguous and simplifies the notation.

Because of spatial homogeneity it is convenient to consider the stochastic equation (19) in terms of the Fourier transform $\rho(\vec{k},t)$ of the density field

$$\frac{\partial\rho(\vec{k},t)}{\partial t}=-k^2D(t)\rho(\vec{k},t)+\eta(\vec{k},t). \tag{22}$$

The formal solution of Eq. (22) reads

$$\rho(\vec{k},t)=\rho(\vec{k},0)e^{-R^2(t)k^2}+\int_0^t\eta(\vec{k},t')e^{[R(t')-R(t)]k^2}. \tag{23}$$

With Eq. (23) the two time correlator can be computed as

$$C(\vec{k},t_w,t)=e^{-[R^2(t_w)+R^2(t)]k^2}\{C(\vec{k},0,0)+T[e^{2R^2(t_w)k^2}-1]\}, \tag{24}$$

where we have made use of the noise field correlations (17).

The whole problem is now reduced to the knowledge of $R(t)$, or, equivalently, of $D(t)$ since $R(t)$ and $D(t)$ are related through Eq. (15). In order to calculate $D(t)=\langle M(\rho)\rangle$ one has to compute averages over the appropriate distribution probability, $\mathcal{P}(\{\rho\},t)$, which obeys the Fokker-Plank equation [11] associated to the Langevin stochastic equation (22). The computation of $D(t)$ can be made as $D(t)=\int_0^1M(\rho)P(\rho)d\rho$, where $P(\rho)$ is given in by

$$P(\rho)=[2\pi S^2(t)]e^{-(\rho-\overline{\rho})^2/[2S^2(t)]}. \tag{25}$$

Then

$$D(t)=[2\pi S^2(t)]^{-1/2}\int_0^1M(\rho)e^{-(\rho-\overline{\rho})^2/[2S^2(t)]}d\rho. \tag{26}$$

With an uncorrelated initial condition $C(k,0,0)=\text{const}$, $S^2(t)$ can be explicitly calculated from Eq. (24) as

$$S^2(t)=h\Delta S^2R^{-d}(t)\Phi_d[\sqrt{2}\Lambda R(t)]+qT, \tag{27}$$

where $\Phi_d[x]=\int_0^x y^{d-1}\exp(-y^2)dy$, $q=(\Sigma_d/d)[\Lambda/(2\pi)]^d$, $h=[d/(\Lambda\sqrt{2})^d]$, Σ_d is the surface of the d-dimensional unitary hypersphere, and $\Delta S^2=S^2(0)-qT$ is the difference between the density fluctuations in the initial and final states. Since the characteristic fluctuations present in the equilibrium state S^2_{eq} are an increasing function of the temperature, for deep quenches, one can have a rather different value of this quantity between the initial and the final state. This fact, as will be shown, can produce a markedly out-off-equilibrium dynamical pattern in the preasymptotic time domain. Notice that the asymptotic value of the density fluctuations $S^2(\infty)=qT$ vanishes at the point of structural arrest $\overline{\rho}=1$ [since the rescaled temperature vanishes according to Eq. (21)].

Equations (15), (26), (27) are a closed set of equations that will be studied analytically in Sec. VI. From Eq. (24) the normalized correlator (10) is given by

$$\tilde{C}(\vec{k},t_w,t)=e^{-[R^2(t)-R^2(t_w)]k^2}. \tag{28}$$

This expression obeys a definite scaling form $\tilde{C}(\vec{k},t_w,t)=\mathcal{S}[\phi(t)/\phi(t_w)]$, with $\phi(t)=\exp\{-R^2(t)k^2\}$, as suggested in the framework of a scaling approach to dynamical processes proposed in Refs. [12,13]. The spatially averaged autocorrelation obeys

$$A(t_w,t)=(4\pi)^{-d/2}[R^2(t)-R^2(t_w)]^{-d/2}. \tag{29}$$

VI. SOLUTION OF THE MEAN FIELD MODEL

A. Evaluating the effective diffusivity $D(t)$

The integral on the left-hand side of Eq. (26) can be evaluated asymptotically by the steepest descent technique since the integrand function in Eq. (26) is peaked around $\rho_M(t)$ given by

$$(1-\rho_M)^2(\overline{\rho}-\rho_M)=vS^2(t). \tag{30}$$

Notice that $\rho_M(t)$ approaches the average density $\overline{\rho}$ from below. This is intuitive because basically $\rho_M(t)$ represents the typical density which drives the dynamics, and this is initially dominated by the evolution of less dense regions, the denser being almost frozen. We consider two limiting cases: (i) $\overline{\rho}-\rho_M(t)\gg 1-\overline{\rho}$ and (ii) $\overline{\rho}-\rho_M(t)\ll 1-\overline{\rho}$.

(i) $\overline{\rho}-\rho_M(t)\gg 1-\overline{\rho}$. In this case one has

$$\overline{\rho}-\rho_M(t)\simeq[vS^2(t)]^{1/3}. \tag{31}$$

Enforcing the condition (i) one sees that the domain of applicability of this solution is

$$S^2(t)\gg\frac{1}{v}(1-\overline{\rho})^3. \tag{32}$$

The saddle point evaluation of the integral in Eq. (26) leads to

$$D(t)\simeq\exp\left[-\frac{3v^{2/3}}{2S^{2/3}(t)}\right]. \tag{33}$$

(ii) $\overline{\rho}-\rho_M(t)\ll 1-\overline{\rho}$. From Eq. (30) one has

$$\overline{\rho}-\rho_M(t)\simeq\frac{vS^2(t)}{(1-\overline{\rho})^2} \tag{34}$$

which holds when

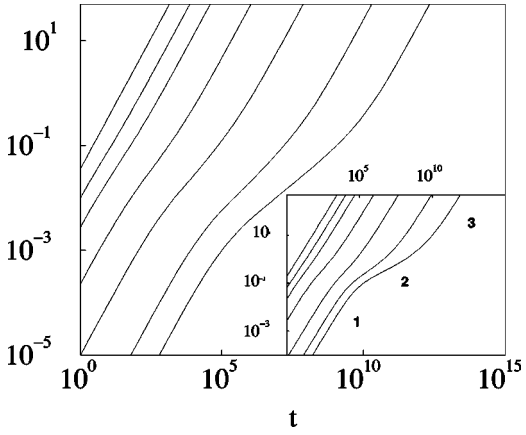

FIG. 1. The evolution of the particles mean square displacement $R^2(t)$, obtained numerically by means of Eq. (15), is plotted for a quench to $T=10^{-4}$ and different densities ($\bar{\rho}=0.70$, 0.80, 0.85, 0.90, 0.93, 0.95, from top to bottom). In the inset the mean field behavior, corresponding to the same parameters, is shown. The location of the three regimes described in the text are outlined by the numbers 1, 2, and 3

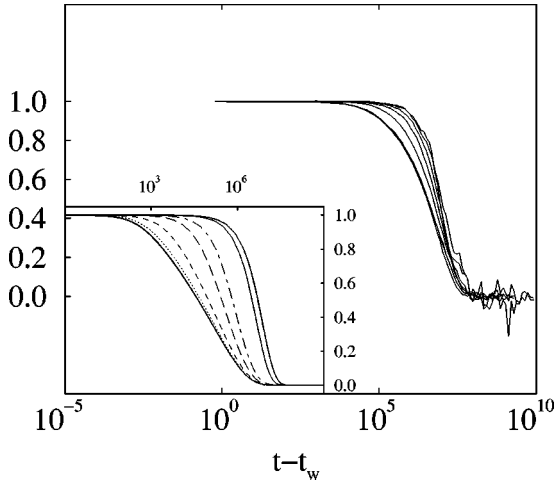

FIG. 2. The decay of $\tilde{C}(\vec{k},t_w,t)$ for a quench to $T=10^{-4}$ with $\bar{\rho}=0.95$ is shown. Different t_w are shown ($t_w=1,10^4,10^5,10^6,10^7,10^9,10^{11},10^{13}$, from left to right). The inset refers to the mean field behavior, with the same choice of parameters.

$$S^2(t) \ll \frac{1}{v}(1-\bar{\rho})^3. \tag{35}$$

With the solution (34), Eq. (26) leads to

$$D(t) \simeq \exp\left[\frac{v}{\bar{\rho}-1}\right]. \tag{36}$$

B. Three dynamical regimes

From the solution of the mean field model one shows the existence, for deep quenches with an high density, of three distinct regimes. We consider them separately below.

1. Regime 1: Pinning

From Eq. (24) it is readily seen that $\partial C(\vec{k},t,t)/\partial t$ is maximum at $k^2=k_M^2=1/[2R^2(t)]$ and it is negligible for $k^2 \ll k_M^2$. For small t, $\partial C(\vec{k},t)/\partial t$ is negligible in the whole physical range $|k|<\Lambda$, so that practically no evolution is observed and the system looks pinned for times shorter than a characteristic value τ_p (to be described in details later on). Since this is an initial regime we also have $\Phi_d[\sqrt{2}\Lambda R(t)] \sim R(t)^d$, and consequently $S(t)\simeq S(0)$ and $D(t)\simeq D(0)$.

Notice that, although the spatial configuration of the coarse grained field is not appreciably changing in this time domain, the mean square displacement $R^2(t)$ grows as

$$R^2(t) \simeq D(0)t \tag{37}$$

(see Fig. 1). At first sight the fact that this frozen state manifests itself with the constancy of all the physical observables but one can seem unphysical, since one would expect also $R^2(t)$ to be a constant. However, it must be observed that $R^2(t)-R^2(t_w) \ll \Lambda^{-2}$ in this regime, and that Λ^{-1} is the typical size over which the variable ρ is coarse grained. In an hard sphere system this would correspond to a movement of the particles over distances smaller than the cage size a. When the density is sufficiently high particles rattle many times inside the cages formed by the neighbors. Since ρ is a coarse grained variable describing the structural relaxation, however, it is not influenced by this small-scale evolution [the same considerations apply to the observables $C(\vec{k},t_w,t)$ and $S(t)$ as well]. The first regime, then, is essentially due to a *cage effect*. The increase of $R^2(t)$ will eventually produce the breakdown of this pinned state. Then the evolution of the coarse grained variable $\rho(\vec{r},t)$ starts and different dynamical regimes occur. These considerations clarify that the present model describes the structural rearrangements of the material but not the small scale evolution inside the cages.

It must be noticed that the existence of a cage effect influences the dynamics at any generic time, even after τ_p, as can be monitored by inspection of the two-time correlations. From Eq. (28), in fact, one has that $\partial \tilde{C}(\vec{k},t_w,t)/\partial t$ is maximum at $k^2=k_M^2=1/[R^2(t)-R^2(t_w)]$ and it is negligible for $k^2 \ll k_M^2$. For $R^2(t)-R^2(t_w) \ll \Lambda^{-2}$, $\partial \tilde{C}(\vec{k},t_w,t)/\partial t$ is negligible in the whole physical range $|k|<\Lambda$, and the two-time correlator stays constant, as shown in Fig. 2, despite the system is not pinned for $t_w > \tau_p$.

2. Regime 2: Slow evolution

Pinning lasts up to τ_p. For $t>\tau_p$, we have $R(t)>\Lambda^{-1}$, thus particles diffuse out of the cages and the evolution starts. For sufficiently deep quenches and large densities, condition (32) applies in an intermediate time domain. Moreover, in this case, ΔS^2 is much larger then the fluctuation of the low-temperature final state $S(\infty)=qT$, so that the last term in Eq. (27) can be neglected. Therefore, using the determination (33) of the diffusivity $D(t)$ in connection with Eqs. (15),(27) we arrive at the following equation for $R(t)$:

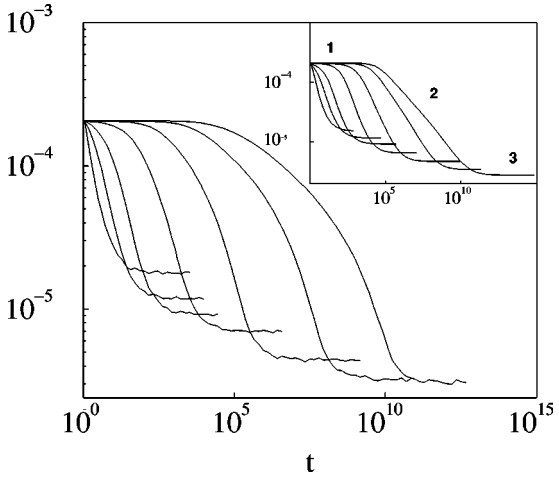

FIG. 3. The density fluctuations $S^2(t)$ are plotted against time for different densities ($\bar{\rho}=0.70$, 0.80, 0.85, 0.90, 0.93, 0.95 from left to right) for a quench to $T=10^{-4}$. In the main frame the outcome of a numerical simulation of Eq. (5) is shown whereas the inset refers to the mean field solution, with the same parameters. The location of the three regimes described in the text are outlined by the numbers 1, 2, and 3.

$$\frac{dR^2(t)}{dt}=\exp\left\{-3\left(\frac{v}{h\Delta S^2}\right)^{2/3}\frac{R(t)^{-2d/3}}{\Phi_d[\sqrt{2}\Lambda R^2(t)]}\right\}. \quad (38)$$

Solving for long times one has

$$R^2(t)\simeq b(\ln t)^{\delta} \quad (39)$$

with $\delta=6/d$ and

$$b=\left[\frac{\Phi_d(\infty)(h\Delta S^2)^{2/3}}{3v^{2/3}}\right]^{6/d}. \quad (40)$$

By virtue of Eq. (24) this implies that, for fixed t_w, the correlator decays as an enhanced power law (see Fig. 2)

$$\tilde{C}(\vec{k},t_w,t)=\exp\{R^2(t_w)k^2\}\exp\{-b[\ln(t)]^{\delta}k^2\}. \quad (41)$$

When also $t_w>\tau_p$, one has

$$\tilde{C}(\vec{k},t_w,t)=\exp\{-b([\ln(t)]^{\delta}-[\ln(t_w)]^{\delta})k^2\}. \quad (42)$$

From Eq. (42) it is readily seen that $\tilde{C}(\vec{k},t_w,t)$ is not a function of the difference $t-t_w$ alone, but depends separately on t_w and t. Time translational invariance is not obeyed in this regime, as shown in Fig. 2.

From Eqs. (27),(39), $S(t)$ can be obtained as

$$S(t)\sim(\ln t)^{-3/2} \quad (43)$$

(see Fig. 3). A logarithmic relaxation of the density fluctuations is also observed in molecular dynamics simulations of out of equilibrium liquid glass former [14]. From Eqs. (11),(39) the spatially averaged autocorrelation $A(t_w,t)$ also decays logarithmically.

Physically, during the second regime the system manages in order decrease the large fluctuations seeded by the high temperature initial condition. However, this is a complicated task, since the dynamics is slaved to the slow evolution of the dense region that are almost frozen. Eventually, when the fluctuations $S(t)$ become comparable to their equilibrium value, this regime ends and the third, stationary, state is entered at $t=\tau_e$.

3. Regime 3: Equilibrium

For long times, $t>\tau_e$, a simple diffusive behavior is obtained because $D(t)$ attains asymptotically a constant value $D(\infty)$, as can be easily checked from Eq. (26). This implies

$$R^2(t)\simeq D(\infty)t \quad (44)$$

as can be seen in Fig. 1, so that the normalized correlator exhibits the usual exponential decay as a function of t

$$\tilde{C}(\vec{k},t_w,t)=e^{-D(\infty)tk^2}e^{\{R^2(t_w)k^2\}} \quad (45)$$

(see Fig. 2). When $t_w>\tau_e$, one has

$$\tilde{C}(\vec{k},t_w,t)=e^{-D(\infty)[t-t_w]k^2} \quad (46)$$

and time translational invariance is obeyed.

C. Characteristic times

For shallow quenches and small densities the duration of the preasymptotic regimes (1 and 2) is negligibly small and the equilibrium state is entered from the beginning. This duration increases if the system is initially brought very far away from equilibrium by performing deep quenches with a high density $\bar{\rho}$. The role of the temperature jump ΔT is obvious, since increasing ΔT brings the initial and final states far away. On the other hand, dense regions, which are initially frozen, are more abundant when $\bar{\rho}$ is increased towards 1, thus slowing the dynamics. Here we make these considerations more quantitative by explicitly computing the typical duration τ_p and τ_e of these regimes. In Fig. 8 (inset) these characteristic durations obtained from a numerical integration of the mean field equations are shown.

Moreover, we will also compute the characteristic time of relaxation of fluctuations $\tau^{\rm rel}$ in the three kinetic regimes. This relaxation time can be computed from the knowledge of $\tilde{C}(\vec{k},t_w,t)$ since, from Eq. (28), $\tilde{C}(\vec{k},t_w,t)$ is a function which monotonously decays over a characteristic time interval $\tau^{\rm rel}(k,t_w)$ defined through

$$R^2(\tau^{\rm rel}+t_w)-R^2(t_w)=k^{-2}. \quad (47)$$

1. Regime 1: Pinning

The duration τ_p of this first regime can be obtained by requiring $\partial C(\vec{k},t,t)/\partial t$ to be negligible in the physical range $|k|<\Lambda$. We compute $\partial C(\vec{k},t,t)/\partial t$ from Eqs. (24),(37) as

$$\frac{\partial C(\vec{k},t,t)}{\partial t} = -2k^2 D(0)[C(\vec{k},0,0) - T]e^{-2D(0)k^2 t}. \quad (48)$$

For small times the maximum of this function in the physical range $|k| \leq \Lambda$ is located at $k=\Lambda$. The requirement that $\partial C(|k|=\Lambda,t,t)/\partial t$ must be small can be fulfilled up to a certain time [15]

$$\tau_p \simeq \frac{\ln\{2\Lambda^2 D(0)\}}{2\Lambda^2 D(0)} \left\{ 1 + \frac{\ln[q\Delta S^2]}{\ln[2\Lambda^2 D(0)]} \right\}, \quad (49)$$

where the constant q and the difference ΔS^2 between the density fluctuations in the initial and final states have been defined below Eq. (27). τ_p depends both on the density $\overline{\rho}$ and T_i through $D(0)$ [see Eq. (26)] and on the quench depth through ΔS^2. When both T_i and T are held fixed, so that $\Delta S^2 = \text{const}$, τ_p grows as $D(0)^{-1}$ as the density is increased. The explicit dependence $D(0)$ on $\overline{\rho}$ can be estimated in simple limiting cases. For large values of T_i, since the thermal fluctuations of the initial state are large, condition (32) applies and, from Eq. (33) one has

$$D(0) \simeq \exp\left[-\frac{3v^{2/3}}{2(1-\overline{\rho})^{2/3}} \right] \quad (50)$$

since for large T_i one has $S(0) \simeq 1 - \overline{\rho}$. For sufficiently small T_i, so that condition (35) applies, $D(0)$ can be evaluated through Eq. (36)

$$D(0) \simeq \exp\left[\frac{v}{\overline{\rho} - 1} \right]. \quad (51)$$

In both cases (50),(51) one observes a strong divergence of $\tau_p(k)$ as the maximum density is approached.

On the other hand, for fixed $\overline{\rho}$ and T_i, so that $D(0) = \text{const}$, τ_p depends logarithmically on the density difference ΔS^2, which increases as the quench depth is increased. Notice that, for $\Delta S^2 < [2q\Lambda^2 D(0)]$, pinning is completely absent.

The typical relaxation time in the pinned state $\tau_p^{\text{rel}}(k)$ as defined through Eq. (47), is obtained using Eq. (37) as

$$\tau_p^{\text{rel}}(k) = \frac{1}{D(0)k^2} \quad (52)$$

which does not depend on t_w.

2. Regime 2: Slow evolution

During the slow evolution regime $R(t)$ increases while $S(t)$ decreases. Therefore, after some characteristic time τ_e, at least one of the two conditions we have used to infer the existence of this regime, namely, condition (32) and the negligibility of the last term on the right-hand side of Eq. (27), can no longer be fulfilled. Given the time dependence (43) of $S(t)$ in this stage the equilibration time τ_e is

$$\tau_e = \min\{M^{-1}(\overline{\rho}), \exp(S_{\text{eq}}^2)^{-1/3}\}, \quad (53)$$

where $S_{\text{eq}}^2 = qT$ are the density fluctuations in the equilibrium state. From Eq. (53) it is seen that for very small (fixed) final temperatures, since $\exp(S_{\text{eq}}^2)^{-1/3}$ is very large, $\tau_e \sim M^{-1}(\overline{\rho})$ diverges *á la* Vogel-Fulcher as ρ_c is approached. The mechanism leading to the equilibrium state in this case is an unactivated structural rearrangement of dense regions which takes place at $T=0$ as well. On the other hand, if the density is kept constant to a high value, the equilibration time diverges with decreasing temperatures in a modified Arrhenius form $\tau_e \sim \exp(qT)^{-1/3}$. In this case equilibration is achieved by thermal fluctuations *shaking* the frozen regions and, therefore, is due to an activated mechanism.

The characteristic relaxation time $\tau_s^{\text{rel}}(k,t_w)$ in the slow evolution regime can be computed through Eqs. (39),(47) as

$$\tau_s^{\text{rel}}(k,t_w) = \exp\left[\frac{1}{bk^2} + (\ln t_w)^{\delta} \right]^{1/\delta} - t_w. \quad (54)$$

From Eq. (54) we see that, due to the lack of time translational invariance, the relaxation time depends on t_w. For large waiting times $\tau_s^{\text{rel}}(k,t_w)$ grows linearly with t_w (apart from logarithmic corrections), namely, $\tau_s^{\text{rel}}(k,t_w) \simeq t_w / [\delta b k^2 (\ln t_w)^{\delta}]$. Furthermore, since from Eq. (40) one has $b \sim (\Delta S^2)^{3/d}$, one sees that, for fixed t_w, $\tau_s^{\text{rel}}(k,t_w)$ is a decreasing function of ΔS^2, that is of the quench depth.

3. Regime 3: Equilibrium

The equilibrium relaxation time $\tau_0^{\text{rel}}(k)$ can be easily computed through Eqs. (44),(47) as

$$\tau_0^{\text{rel}}(k) = \frac{1}{D(\infty)k^2} \quad (55)$$

which does not depend on t_w, due to the time translational invariance. At the point of structural arrest the density fluctuation of the equilibrium state vanish, so that, through Eq. (36), one has $D(\infty) \simeq M(\overline{\rho})$. We recover then the Voghel-Fulcher law (1), the relation that has long been known in the literature of viscous fluids and glasses and that was first theoretically obtained by Adam and Gibbs with their *cooperative rearrangement theory*. This justifies *a posteriori* the phenomenological assumption (7) for the mobility.

VII. THE FLUCTUATION-DISSIPATION RATIO

An important issue to understand the off-equilibrium dynamics is the relation between the correlation function in the unperturbed situation, $C(\vec{k},t_w,t)$, and the response function of the system to a small perturbing external field $h(\vec{r},t)$ coupled via a term $-\int d\vec{r} h\rho$ in the free energy. This leads, instead of Eq. (22), to

$$\frac{\partial \rho(\vec{k},t)}{\partial t} = -k^2 D(t)\rho(\vec{k},t) + k^2 D(t) h(\vec{k},t) + \eta(\vec{k},t) \quad (56)$$

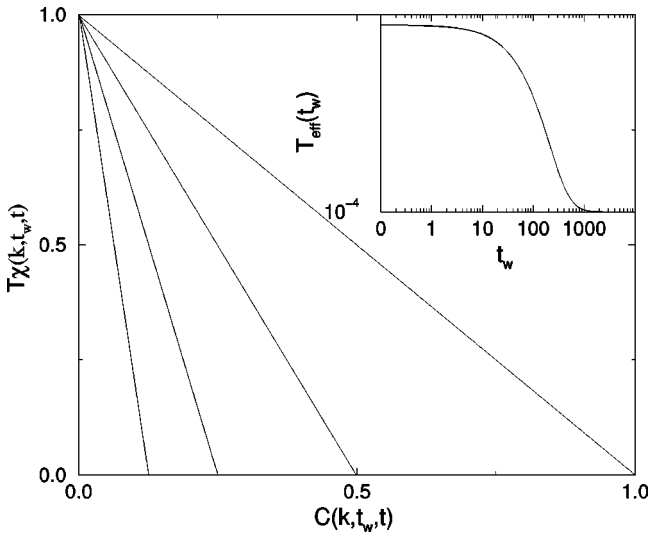

FIG. 4. Fluctuation dissipation plot. The integrated response $\chi(\vec{k},t,t_w)$ is plotted against $C(\vec{k},t,t_w)$ in mean field for $k=\pi/2$ and different waiting times ($t_w=150,230,350,2000$ from left to right). The temperature of the quench is $T=10^{-4}$ and the average density $\overline{\rho}=0.95$. In the inset the time evolution of the *effective* temperature $T_{\rm eff}$ is shown.

so that

$$\rho(\vec{k},t)=\rho(\vec{k},0)e^{-R^2(t)k^2}+\int_0^t[\,\eta(\vec{k},t') + k^2D(t')h(\vec{k},t')]e^{[R(t')-R(t)]k^2}. \quad (57)$$

The integrated response function

$$\chi(\vec{k},t_w,t)\equiv\int_{t_w}^{t}\frac{\delta\rho(\vec{k},t)}{\delta h(\vec{k},t')}dt' \quad (58)$$

reads

$$\chi(\vec{k},t_w,t)=1-\tilde{C}(\vec{k},t_w,t). \quad (59)$$

The quantities χ and C in equilibrium are linked one to the other since the fluctuation-dissipation theorem [16] states that

$$X\equiv -T\frac{\partial\chi(\vec{k},t_w,t)}{\partial C(\vec{k},t_w,t)}=1. \quad (60)$$

In off-equilibrium situations this relation is violated and, generally, X, the fluctuation dissipation ratio, is a function of t and t_w [17].

In the present mean-field model, we can readily evaluate X as

$$X(t_w,t)=TC^{-1}(\vec{k},t_w,t_w), \quad (61)$$

namely, the inverse of the structure factor computed at t_w times the bath temperature. The parametric plot of $T\chi$ vs C (fluctuation dissipation plot) is shown in Fig. 4; for every t_w it is represented by a straight line whose slope slowly approaches 1 when t_w grows, suggesting that $T_{\rm eff}=TX^{-1}$ plays the role of an *effective* temperature [18] slowly approaching the bath temperature from above. Notice that X depends on t_w alone. This feature can be compared with recent investigations of the response of supercooled liquids in molecular dynamic simulations. In Ref. [19] a similar behavior with a t_w-dependent *internal* temperature is observed for the *intrabasin* response, namely, for large $t-t_w$, of a Lennard-Jones binary mixture. For small $t-t_w$ the response proves the *intrabasin* vibrational dynamics, in equilibrium at the bath temperature, which, in the present approach, is integrated out by the coarse-graining procedure. Interestingly, in the study of fluctuation-dissipation relations and violations of the equilibrium FDT, a function X depending only on t_w has also been found in models for granular media [20] and in experiments on structural glasses [21].

VIII. NUMERICAL SOLUTION: METHODS AND RESULTS

We now proceed to the study of Eq. (5) by means of numerical simulations. We have integrated Eq. (5) in the presence of the mobility (7) on a two-dimensional square lattice with mesh size Δx and periodic boundary conditions in all directions [22]. Both spatial derivatives and time integration have been approximated by an Euler first order discretization scheme.

Regarding time discretization, since the density fluctuations are initially very large, due to the high-temperature initial condition, a small value of dt is required at the beginning of the simulation in order to avoid numerical instabilities. However, for longer times, fluctuations decay (see Fig. 3) and larger values of dt can be used. Moreover, for dense systems, the degree of instability of Eq. (5) is greatly tamed by the smallness of $M(\rho)$. The value of dt can therefore be adjusted according to the average density $\overline{\rho}$. The speed of the computation, then, can be greatly enhanced by selecting a appropriate initial dt for each value of $\overline{\rho}$ and then using an adaptive time step technique that successively increases it properly as time goes on. With this trick very long relaxation times for high density systems can be accessed. For spatial discretization we simply take $\Delta x=1$.

The presented results have been obtained by averaging over ten different initial configurations for lattice size $L=128$. The sample is quenched rapidly from high temperature to the working temperature T which is reached at time $t=0$. The initial condition $\rho(\vec{r},t)$ which describes the homogeneous state with random fluctuations at a very high temperature before the quench is given by $\rho(\vec{r},t)=\overline{\rho}+\delta\rho(\vec{r},t)$, where $\overline{\rho}$ is the average density, which will remain constant during time evolution, and $\delta\rho(\vec{r},t)$ are random numbers uniformly distributed in $[0,1-\overline{\rho}]$. The system is subsequently allowed to evolve at constant temperature T according to Eq. (5).

We present results for different temperatures and average densities $\overline{\rho}$. The behavior of samples with different $\overline{\rho}$ shows

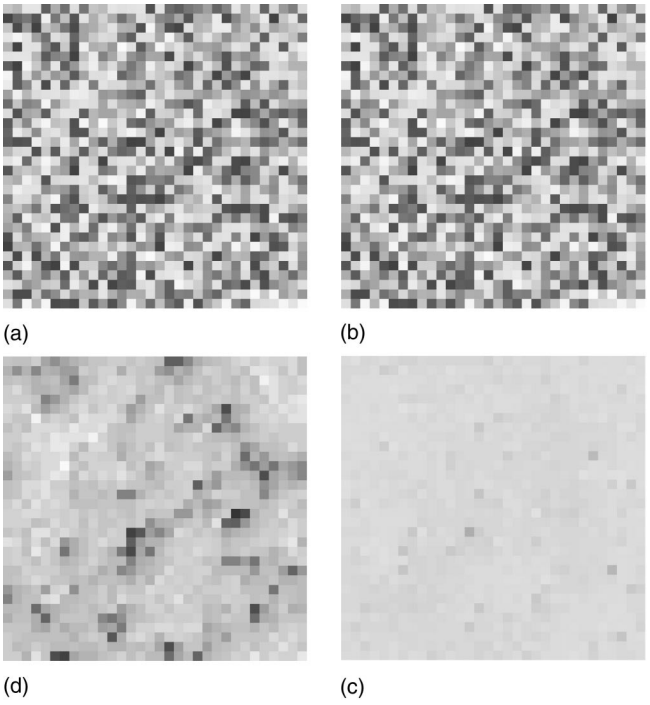

FIG. 5. Snapshots of the local densities in the system shown at different times from the quench instant onward, for $\bar{\rho}=0.95$ and $T=10^{-4}$. Parts of the figure referred to as (a)–(d) are counted clockwise starting from top-left. Dark spots are denser regions. (a) shows the initial high-temperature disordered configuration, characterized by large density fluctuations. As time goes on, the system is practically pinned in the initial configuration up to a characteristic time $\tau_p=750$ (b). This is the first dynamical regime. For $t>\tau_p$, less dense regions equilibrates whereas high density zones are still practically frozen and pronounced spatial heterogeneities are observed. This is shown in (c), where the configuration at the time $t=10^8$, belonging to the second regime, is shown. Only after long times the systems becomes spatially uniform again and equilibrium is attained, as show in (d) at $t=10^{12}$.

that, for densities up to $\bar{\rho}\simeq 0.7$ a simple diffusive behavior is observed, corresponding to a *normal liquid* region. Here the mobility remains of order 1 all over the system. In this case the behavior of all the observables introduced in Sec. IV can be computed analytically by letting $M(\rho)=\text{const}$ in Eq. (5); we have tested this hypothesis numerically. The decay of the average density fluctuations $S^2(t)$, for instance, is plotted in Fig. 3. For low densities $S^2(t)$ very quickly decays to the constant value characteristic of the equilibrium state. The mean square displacement $R^2(t)$, shown in Fig. 1, behaves linearly and the autocorrelation function $\tilde{C}(\vec{k},t_w,t)$ of the system has an exponential decay, as expected for a simple liquid.

By raising the density, one gradually enters a different regime where the vanishing of the mobility slows the dynamics: this produces an off equilibrium glassy behavior, before the equilibrium state is entered, that becomes more evident as density is increased toward $\bar{\rho}=1$. The behavior of $S^2(t)$ shows that, for large densities, the dynamics can be divided in three regimes. Initially, for t smaller than a characteristic time τ_p, $S^2(t)$ remains constant. This is the first regime.

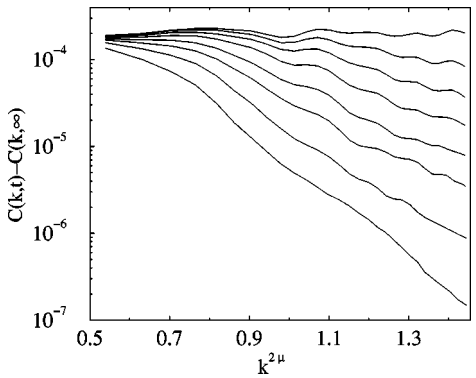

FIG. 6. The spatial heterogeneous pattern in the *slow regime* (c) is outlined by a slow decay, as a function of k, of the structure factor $C(\vec{k},t)$, plotted here against $k^{2\mu}$, with $\mu=1/6$. $C(\vec{k},t)$ is consistent with a non-Gaussian fit: $C(\vec{k},t)\simeq \mathcal{C}e^{-[l(t)k]^{2\mu}}$. Different curves from top to bottom refer to increasing times belonging to the second regime, with $\bar{\rho}=0.95$ and $T=10^{-4}$.

Then, for $t>\tau_p$, a second regime is entered characterized by the decrease of $S^2(t)$. Eventually equilibrium is achieved and $S^2(t)$ reaches a constant value.

This whole pattern is reflected in the behavior of the particle mean square displacement $R^2(t)$, which is plotted in Fig. 1. As the density is increased toward the limiting value $\rho_c=1$, the behavior of $R^2(t)$ shows evident deviations from a linear growth typical of Brownian motion. In the first regime $R^2(t)$ grows linearly in time. The inflection region in the intermediate time domain corresponds to the second regime. This becomes more pronounced when the density is increased. Then, in the equilibrium state, $R^2(t)$ keeps growing linearly again. The three dynamical regimes characteristic of dense systems will be discussed in detail separately below.

A. Regime 1: Pinning

Let us consider the *snapshots* pictures, as those presented in Fig. 5, showing the system during the dynamical evolution. In this figure the configuration of a system with $\bar{\rho}=0.95$ quenched from an high temperature initial state to $T=10^{-4}$ is shown at different times. Here the gray scale corresponds to the value of the density $\rho(\vec{r},t)$, the darker regions being the denser [black corresponds to $\rho(\vec{r},t)=1$]. The first plot represents the system in the initial high-temperature state at time $t=0$ while the second picture shows the situation at time $\tau_p=750$. From the observation of these two figures one sees that initially, for times up to τ_p, the system is blocked and practically no evolution is observed. Large density fluctuations, seeded in by the high-temperature initial condition, are frozen and the system is trapped. This pinning phenomenon is reflected by the behavior of both $C(\vec{k},t_w,t)$ and $S^2(t)$, as shown in Figs. 2 and 3, respectively, which remain constant in this time domain.

B. Regime 2: Slow evolution

The second regime is entered at $t\sim\tau_p$ and lasts up to $t\sim\tau_e$. The typical configuration of the system in this time

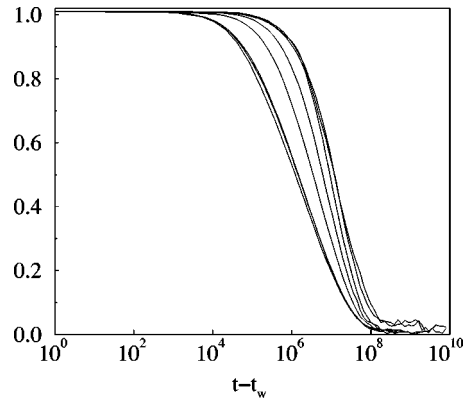

FIG. 7. $A(t,t_w)$ is plotted against $t-t_w$ for different values of t_w (increasing from left to right), at $\overline{\rho}=0.95$ and $T=10^{-4}$.

domain corresponds to the picture in the third column of Fig. 5. Here one observes that less dense regions equilibrate whereas high density zones are still practically frozen. After a while this gives rise to pronounced correlated spatial heterogeneities. This spatial pattern is outlined by a slow decay, as a function of k, of the structure factor $C(\vec{k},t)=\langle\rho(\vec{k},t)\rho(-\vec{k},t)\rangle$, that is consistent with a stretched exponential fit:

$$C(\vec{k},t)\simeq\mathcal{C}e^{-[l(t)k]^{2\mu}} \tag{62}$$

with $\mu\simeq 1/6$ (at variance with the usual Gaussian decay of standard diffusion), as shown in Fig. 6. Dynamical heterogeneities are related to cooperative rearrangements of particles in glassy states owing to configurational restrictions. Such an idea was first put forth by Adam and Gibbs [8] who introduced the idea of cooperatively rearranging regions. In this second regime the kinetics, in fact, is ruled by the constrained evolution of spatial heterogeneities with large ρ, which produce a *slow* dynamics. The two time correlators $C(k,t_w,t)$ and $A(t,t_w)$, shown in Figs. 2 and 7 decay correspondingly more slowly than an exponential. Moreover one sees that time translational invariance is lacking since a sensible dependence on the waiting time t_w is observed. In Fig. 8 τ_p and τ_e obtained through the numerical solution of the model are plotted as function of the density: the behavior of the relaxation times is consistent with an exponential divergence, as found in mean field.

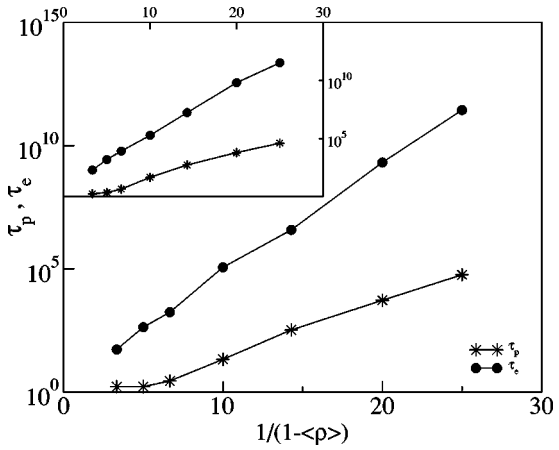

FIG. 8. The characteristic times τ_p and τ_e are plotted against $1/(1-\overline{\rho})$ for $T=10^{-4}$. The main picture refers to the numerical calculations while in the inset the mean field behavior is shown.

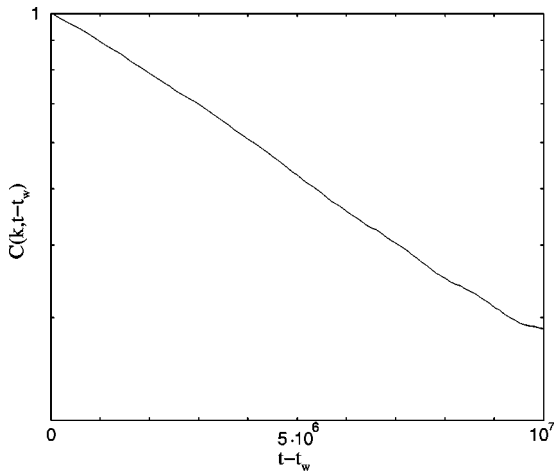

FIG. 9. $C(k,t,t_w)$ is plotted in the equilibrium regime against $t-t_w$ for $\overline{\rho}=0.95$, $T=10^{-5}$.

1. Regime 3: Equilibrium

After a characteristic time τ_e, the strong spatial heterogeneities observed in the second regime decay and the system enters an asymptotic stage characterized by small temperature fluctuations around the average density $\overline{\rho}$, as shown in Fig. 5. This regime corresponds to an equilibrated state where time translational invariance is obeyed and the autocorrelation function decays exponentially, as shown in Fig. 9.

IX. CONCLUSIONS

In this paper we have studied the schematic model introduced in Ref. [1] for the description of the out of equilibrium kinetics of supercooled fluids and glassy systems above the temperature of structural arrest. It consists of a diffusion equation with a mobility in the manner of Vogel-Tamman-Fulcher in contact with a thermal bath. A detailed analysis has been carried out both analytically in a mean field approach and numerically. The main result is the characterization of the gradual crossover between a *normal liquid* behavior, where a simple diffusive relaxation with exponentially damped correlations is found, and a glassy behavior where the existence of heterogeneities produces strong off-equilibrium effects. Some properties that are observed in systems close to the glassy transition, such as the existence of strong spatial heterogeneities, anomalous diffusion, slow decay (such as enhanced power law), aging of density autocorrelation functions, a non trivial fluctuation dissipation ratio $X(t_w)$, dynamical scaling with time, are exhibited by the model.

The relative simplicity of the model allows us to make rather precise quantitative predictions which could be, in

principle, tested in experiments on glassy systems. Moreover, the model can be generalized in a rather straightforward way to study the effect of a gradual cooling procedure (this is the situation generally achieved in experiments), or to investigate the dynamics of a supercooled fluid subject to an external drift, such as a shear flow [23].

ACKNOWLEDGMENTS

We thank D. Del Vecchio for a critical reading of the manuscript. F.C. thanks M. Cirillo and R. Del Sole for the hospitality at Rome University, and M. Palummo for computer help. This work was supported with the TMR network Contract Nos. ERBFM-RXCT980183 and PRA-HOP 1999 INFM.

APPENDIX A: THE COARSE GRAINED FREE ENERGY

We consider an assembly of particles of typical size l and density $\overline{\rho}$, with an hardcore repulsive interaction, randomly moving on a d-dimensional space. Although particles move continuously in time and space one can introduce an approximation by assuming the existence of a lattice and requiring that, due to the hardcore interaction, the occupation number of each lattice site can only take the values 0,1. This gas-lattice model can be described in terms of a coarse-grained variable $\rho(\vec{r})$ representing the average particle density inside a box of typical size a centered at $\vec{r}$. Since particles do not interact, the only contribution to the free energy of this system comes from the entropy S. Let us consider a box containing N lattice sites. Classically the number of distinguishable way for $n(\vec{r})$ particles to occupy the box is given by

$$g(\vec{r})=\frac{N!}{n(\vec{r})![N-n(\vec{r})]!}. \tag{A1}$$

Then the contribution $S(\vec{r})$ to the total entropy coming from the box is

$$S(\vec{r})=\ln\frac{N!}{n(\vec{r})![N-n(\vec{r})]!}. \tag{A2}$$

For large N, using the Stirling approximation, the entropy per lattice site $s(\vec{r})=S(\vec{r})/N$ reads

$$s(\vec{r})\simeq-\rho(\vec{r})\ln\rho(\vec{r})-[1-\rho(\vec{r})]\ln[1-\rho(\vec{r})], \tag{A3}$$

where we have used $\rho(\vec{r})=n(\vec{r})/N$. With Eq. (A3) the free energy $F\{\rho\}$ is obtained through

$$\frac{F\{\rho\}}{T}=\int d\vec{r}\{\rho(\vec{r})\ln\rho(\vec{r})+[1-\rho(\vec{r})]\ln[1-\rho(\vec{r})]\}, \tag{A4}$$

where T is the absolute temperature.

The lattice-gas approximation is a reasonable assumption if (i) the lattice constant Δx is larger then l and (ii) the density of the particles is small. Condition (i) allows one to identify the position of a particle with a single site. In this case the approximation amounts to neglecting the details of the spatial distribution of the particles on scales smaller than Δx: This is appropriate when the mean free path λ of the particles is large as compared to Δx that is for small densities. This leads to condition (ii). For high particle concentration, on the other hand, $\lambda \ll l$, so that the details of the particle spatial distribution on scale smaller then Δx becomes relevant. In this case conditions (i) and (ii) cannot be contemporary fulfilled and the approximation, in principle, breaks down. In particular Eq. (8) ceases to be valid. Nevertheless, in the following we will still retain the free energy Eq. (8), since we expect that the far-from-equilibrium properties of the system can be well described, provided a suitable form of the mobility, as discussed in Appendix B, is assumed.

APPENDIX B: A DERIVATION OF ADAM-GIBBS MOBILITY

A functional form of the mobility has been obtained in different approximations by several authors in apparently heterogeneous context as the free-volume theory of the glass transition or ''car-parking'' problems in one dimension [5,6,8]. Here we show a simple argument from free-volume theories, in a spirit very similar to the work by Boutreaux and de Gennes [6].

Let us consider again the hard spheres system introduced before. The ''free volume'' can be defined as the excess of volume which can be redistributed in a box, with a given density, by rearranging particles positions. The average free volume per particle is

$$V_f=\frac{1-\rho(\vec{r})}{\rho(\vec{r})}. \tag{B1}$$

We can now make the reasonable hypothesis that the distribution $\Pi(V)$ of empty spaces V decays exponentially on scales of order V_f

$$\Pi(V)=\frac{1}{V_f}e^{-V/V_f}. \tag{B2}$$

Now we can estimate the probability $M\{\rho\}$ of a particle to make a move at a given time, considering that it cannot enter regions of empty space smaller that its own volume b, as

$$M\{\rho\}=\int_b^\infty \Pi(V)dV=e^{-b/V_f}=e^{-b\rho/(1-\rho)}. \tag{B3}$$

Notice the essential singularity at $\rho=1$ caused by the denominator in the exponent. Since the density dependence of the numerator, instead, does not produces sensible differences we will replace it with a constant, for simplicity. We then consider the following form:

$$M\{\rho\}=e^{-v/(1-\rho)}. \tag{B4}$$

With this form of the mobility Eq. (5) specifies the model studied throughout this paper.

[1] F. Corberi, M. Nicodemi, M. Piccioni, and A. Coniglio, Phys. Rev. Lett. **83**, 5054 (1999).
[2] C.A. Angell, Science **267**, 1924 (1995); M.D. Ediger, C.A. Angell, and S.R. Nagel, J. Phys. Chem. **100**, 13 200 (1996).
[3] W. Gotze and L. Sjogren, Rep. Prog. Phys. **55**, 241 (1992).
[4] W. Kob and H.C. Andersen, Phys. Rev. E **48**, 4364 (1993).
[5] E. Ben-Naim, J.B. Knight, and E.R. Nowak, Physica D **123**, 380 (1998).
[6] T. Boutreux and P.G. de Gennes, Physica A **244**, 59 (1997).
[7] J.D. Gunton, M. San Miguel, and P.S. Sahni, in *Phase Transition and Critical Phenomena*, edited by C. Domb and J.C. Lebowitz (Academic Press, London, 1989), Vol. 8.
[8] G. Adam and J.H. Gibbs, J. Chem. Phys. **43**, 139 (1965).
[9] P.N. Segrè, S.P. Meeker, P.N. Pusey, and W.C.K. Poon, Phys. Rev. Lett. **75**, 958 (1995); P.N. Segrè and P.N. Pusey, *ibid.* **77**, 771 (1996); see also citations in Ref. [2].
[10] W. Kob, J.-L. Barrat, Phys. Rev. Lett. **78**, 4581 (1997).
[11] J. Zinn-Justin, *Quantum Field Theory and Critical Phenomena* (Oxford University Press, New York, 1993).
[12] L.F. Cugliandolo and J. Kurchan, J. Phys. A **27**, 5749 (1994).
[13] M. Nicodemi and A. Coniglio, Phys. Rev. E **59**, 2812 (1999).
[14] U. Mussel and H. Rieger, Phys. Rev. Lett. **81**, 930 (1998); J.L. Barrat and W. Kob, *ibid.* **78**, 4581 (1997); W. Kob and J.L. Barrat, *ibid.* **81**, 931 (1998).
[15] It must be remembered that, due to the time rescaling introduced before the characteristic time τ_p (and all those derived below, namely, τ_s, τ_0, and τ_e) must also be rescaled in the same way.
[16] Kubo, M. Toda, and N. Hashitsume, *Statistical Physics* (Springer-Verlag, Berlin, 1985).
[17] J.P. Bouchaud, L.F. Cugliandolo, J. Kurchan, and M. Mezard, in *Spin Glasses and Random Fields*, edited by A.P. Young (World Scientific, Singapore, 1997).
[18] L.F. Cugliandolo, J. Kurchan, and L. Peliti, Phys. Rev. E **55**, 3898 (1997).
[19] F. Sciortino and P. Tartaglia, e-print cond-mat/0007208.
[20] M. Nicodemi, Phys. Rev. Lett. **82**, 3734 (1999).
[21] T.S. Grigera and N.E. Israeloff, Phys. Rev. Lett. **83**, 5038 (1999).
[22] M. Piccioni, Ph.D. thesis, Naples University ''Federico II,'' Naples, 1999.
[23] F. Corberi, G. Gonnella, and D. Suppa, Europhys. Lett. **52**, 318 (2000).